Smart Structures and Systems, Vol. 4, No. 3 (2008) 279-290

DOI: http://dx.doi.org/10.12989/sss.2008.4.3.279

Estimation of viscous and Coulomb damping from free-vibration data by a least-squares curve-fitting analysis

Wesley C. H. Slemp*, William L. Hallauer, Jr.‡ and Rakesh K. Kapania‡†

Virginia Polytechnic Institute and State University, Blacksburg, Virginia, 24061, USA

(Received January 31, 2007, Accepted May 2, 2007)

Abstract. The modeling and parameter estimation of a damped one-degree-of-freedom mass-spring system is examined. This paper presents a method for estimating the system parameters (damping coefficients and natural frequency) from measured free-vibration motion of a system that is modeled to include both subcritical viscous damping and kinetic Coulomb friction. The method applies a commercially available least-squares curve-fitting software function to fit the known solution of the equations of motion to the measured response. The method was tested through numerical simulation, and it was applied to experimental data collected from a laboratory mass-spring apparatus. The mass of this apparatus translates on linear bearings, which are the primary source of light inherent damping. Results indicate that the curve-fitting method is effective and accurate for both perfect and noisy measurements from a lightly damped mass-spring system.

Keywords: friction oscillator; friction estimation; least-squares; coulomb friction; free vibration.

1. Introduction

This study investigated dynamic modeling of one-degree-of-freedom (1-DOF) mechanical systems that are idealized to possess both viscous and Coulomb damping. The paper presents a method of system identification for damping and natural frequency by least-squares curve fitting that uses all discrete data points of a free-vibration decay. Numerical simulation and an experiment were performed to examine the numerical functioning and accuracy of the method. The curve-fitting method is compared with a method developed by Liang and Feeny (1998) that uses only the local extrema of a free-vibration decay. According to Den Hartog (1931), the four most common types of mechanical damping forces are: "viscous" damping (proportional to velocity), "Coulomb" damping, or dry friction (independent of velocity), "air resistance" (proportional to the square or some higher power of velocity), and "internal hysteresis" (dependent only on the amplitude of motion). We consider here 1-DOF systems in which only the viscous and Coulomb types are present. If damping is assumed to be either ideal viscous alone or ideal Coulomb alone, then there are well-known classical methods for estimating damping coefficients from experimental free-vibration data (Meirovitch 2001).

*Undergraduate Researcher, Corresponding Author, E-Mail: wslemp@vt.edu
‡Adjunct Professor, Department of Aerospace and Ocean Engineering
‡†Professor, Department of Aerospace and Ocean Engineering

It is more difficult, though, if damping is a mixture of viscous and Coulomb. Jacobsen and Ayre (1958) observed that viscous damping dominates at high amplitudes of free-vibration displacement relative to the level at which static sticking occurs, and that kinetic Coulomb friction dominates at amplitudes close to the static-sticking level; they illustrated a method, based upon this observation, for estimating both viscous and Coulomb coefficients. More recently, Liang and Feeny (1998) derived more general methods for estimating the viscous and Coulomb damping coefficients from both free-vibration response and frequency response. Their free-vibration analysis uses the data at local crests and troughs throughout a vibration decay trace; the details of this method are presented in Section 2. Liang and Feeny (2004) also developed an algorithm to identify the damping parameters from frequency-response data. They used the nonlinear solution derived by Den Hartog (1931) for frequency response of a 1-DOF system that has both forms of damping. The Liang-Feeny analysis estimates damping parameters from input-output pairs at resonance for two or more amplitudes of excitation and response.

This paper describes an alternative method to estimate values for both viscous and Coulomb damping from the free-vibration data of a 1-DOF mass-spring system. Section 2 presents both the derivation and details of the method. Section 3.1 presents numerical simulations to evaluate the method's performance. Section 3.2 describes the experimental study in which our method was applied to estimate the damping parameters of a laboratory mass-spring apparatus.

2. Theoretical model

Consider a standard 1-DOF damped mass-spring system with mass m, spring stiffness k, viscous damping coefficient c, and kinetic Coulomb resisting force F_k (subscript k for kinetic). Displacement of the mass is denoted as $x(t)$, velocity as $v(t) = \dot{x}$, and externally applied excitation is $f(t)$. The general equation of motion and initial conditions are:

$$m\ddot{x} + c\dot{x} + kx + F_k \text{sign}(\dot{x}) = f(t) \tag{1a}$$

$$x(0) = X_0; \text{ and } \dot{x}(0) = V_0 \tag{1b}$$

For free vibration $f(t) = 0$. The equation of motion is divided by m and expressed more directly by:

$$\ddot{x} + 2\zeta\omega_n\dot{x} + \omega_n^2 x = -\omega_n^2 x_k \qquad \text{if } \dot{x} > 0 \tag{2a}$$

$$\ddot{x} + 2\zeta\omega_n\dot{x} + \omega_n^2 x = \omega_n^2 x_k \qquad \text{if } \dot{x} < 0 \tag{2b}$$

in which the undamped natural frequency is defined by $\omega_n^2 = \text{k/m}$, the viscous damping ratio ζ is defined by $2\zeta\omega_n = \text{c/m}$, and the effects of kinetic Coulomb friction are included through the Coulomb step displacement $x_k = F_k/k$. Static Coulomb friction can cause vibration to cease at a low but non-zero value of displacement on the order of x_k (Meirovitch 2001); however, we consider here only vibration amplitudes above the threshold of sticking.

While the sign of velocity $\dot{x}$ is constant, a 1-DOF system with both viscous and Coulomb damping acts as a second-order linear oscillator with an externally applied step input. For a given direction of motion, the solution of Eqs. (2) may be found for initial conditions $x(t_0) = X_0 >> x_k > 0$ and $\dot{x}(t_0) = 0$ as simply the superposition of initial-displacement response and step response, both of which are well known. For the first half-cycle of motion, ($\dot{x}<0$), the response is given by:

$$x(t) = (X_0 - x_k)e^{-\xi\omega_d(t-t_0)}\{\cos[\omega_d(t-t_0)] + \xi\sin[\omega_d(t-t_0)]\} + x_k \tag{3}$$

The damped natural frequency is defined as $\omega_d = \omega_n\sqrt{1-\zeta^2}$, and $\xi = \zeta/\sqrt{1-\zeta^2}$, provided that $0\le\zeta<1$. We define $t_0=0$. For each successive half-cycle after the first, Eqs. (2) may be solved with initial displacement given by the final, zero-velocity value from the previous half-cycle; this value occurs at instant t when $\omega_d(t-t_{j-1}) = \pi$, in which we define the instant at the end of the j^{th} half-cycle of displacement as $t_j = j\pi/\omega_d$. A recursion formula may be written for the displacement during each successive half-cycle. The decay continues over each half-cycle until the amplitude falls beneath the threshold of sticking, at which time motion ceases. (However, our analysis does not model this static sticking at the end of a vibration decay.) The initial displacement for the $(j+1)^{th}$ half-cycle is

$$X_j = -[X_{j-1}-(-1)^{j-1}x_k]e^{-\xi\pi} + (-1)^{j-1}x_k, \qquad j=1, 2,... \tag{4}$$

The initial conditions may be applied to Eqs. (2) to derive the general solution for displacement during the j^{th} half-cycle:

$$x(t) = [X_{j-1} - (-1)^{j-1}x_k]e^{-\xi\omega_d(t-t_{j-1})}\{\cos[\omega_d(t-t_{j-1})] + \xi\sin[\omega_d(t-t_{j-1})]\} + (-1)^{j-1}x_k \tag{5}$$

Liang and Feeny (1998) proposed summing Eq. (4) for the j^{th} and $(j+1)^{th}$ values in order to calculate a local value ζ_j for viscous damping. The contribution due to Coulomb damping is eliminated, and the following equation results:

$$-e^{-\xi_j\pi} = \frac{X_j + X_{j+1}}{X_{j-1} + X_j} \tag{6}$$

With ξ_j calculated from Eq. (6), then $\zeta_j = \xi_i/\sqrt{1+\xi_j^2}$, and the local Coulomb step displacement x_{kj} is calculated directly from Eq. (4).

Liang and Feeny (1998) observed that experimental measurement of displacement might include a constant small error. Prior to imposing initial displacement X_0, the experimenter might zero the displacement-sensor output with the mass in a static equilibrium position. However, this is not necessarily the position the mass would occupy if there were zero Coulomb friction, because sticking friction can produce a small static offset. This possible static offset or bias, which we denote as x_ε, is initially unknown. Thus, the quantity actually measured in the vibration decay is

$$y(t) = x_\varepsilon + x(t) \tag{7}$$

Therefore, the j^{th} measured local extreme displacement (crest or trough) is denoted as $Y_j = x_\varepsilon + X_j$. Liang and Feeny arithmetically eliminated bias x_ε by differencing measured local extreme values: $Y_p-Y_q = X_p-X_q$, in which p and q are any integers denoting extrema within the non-sticking part of the vibration decay. Next, they arithmetically removed kinetic Coulomb step displacement x_k by summing the equations for $Y_{j+1}-Y_j$ and $Y_j - Y_{j-1}$ to produce the following equation for local ξ_j as an alternative to Eq. (6), in recognition of the possibility of bias x_ε:

$$-e^{-\xi_j \pi} = \frac{Y_{j+1} - Y_{j-1}}{Y_j - Y_{j-2}} \tag{8}$$

With ξ_j determined from Eq. (8), either the equation for $Y_{j+1} - Y_j$ or that for $Y_j - Y_{j-1}$ is applied to calculate the associated local value x_{kj} of Coulomb step displacement.

For light damping, Eq. (8) is inherently vulnerable to experimental error, because both numerator and denominator of the fraction normally involve small differences of close large values. The most extensive data presented by Liang and Feeny (2004) seem to reflect this vulnerability. They averaged damping values calculated from 17 separate free-vibration decays, with two local applications of Eq. (8) per decay over only five observable extrema. Their averaged value of ζ was 0.082, but the local values varied greatly from 0.061 to 0.108; their averaged value of x_k was 0.81 mm, but the local values varied greatly from 0.51 mm to 1.01 mm.

The Jacobsen-Ayre method (1958) and the Liang-Feeny method use only the data from crests and troughs, but no data from the response between those local extrema. In our approach, on the other hand, all discrete data values from measured decay traces are used in the curve fit. The damping parameters ζ and x_k, and the other parameters ω_n, X_0 and x_ε as well, are determined such that the least-squares error between the measured and predicted data is minimized. The minimization is expressed as:

$$\min\left(\sum_{i=0}^{N} [y(t_i) - y_{meas}(t_i)]^2\right) \tag{9}$$

The theoretical model for $y(t_i)$ consists of Eqs. (3)-(5), and (7). N is the total number of data points in the time series of a decay record. An iterative technique is necessary to minimize the function in Eq. (9).

To determine the best-fit parameters ζ, x_k, ω_n, X_0, and x_ε, we applied the function LSQCURVEFIT from the Optimization Toolbox of MATLAB[a] 6, Release 12. From MATLAB's online documentation, the algorithm of LSQCURVEFIT is a "subspace trust region method and is based on the interior-reflective Newton method" described by Coleman and Yi (1996). To minimize the function of Eq. (9), we provided the following inputs to LSQCURVEFIT: a function M-file representing the theoretical model for $y(t_i)$; an initial-estimate 5×1 array of the minimization parameters ζ, x_k, ω_n, X_0, and x_ε, an estimate based primarily on a brief visual inspection of the vibration-decay trace; the experimental data, consisting of an N×1 array of discrete sampling times and the corresponding array of discrete displacement values; a 5×1 array of lower-bound constraints for the minimization parameters; and a 5×1 array of upper-bound constraints. We found that LSQCURVEFIT functioned very well and converged accurately except when we provided intentionally misleading initial estimates. LSQCURVEFIT was mostly insensitive to our lower-bound and upper-bound constraints. However, we always imposed lower-bound constraints of zero on parameters ζ, x_k, and ω_n in order to narrow the search window and to prevent physically impossible negative values for inherent damping and natural frequency.

3. Results of numerical simulations and experiments

Both numerical and experimental studies were performed, utilizing least-squares curve fitting. The numerical simulation was performed to evaluate the accuracy of the method and to study the effects of

[a]MATLAB is a registered trademark of The MathWorks, Inc.

uncertainty in the data. The curve-fitting method was then applied to experimentally measured data from an inherently damped mass-spring system.

3.1. Numerical simulations

For the numerical simulation, the natural frequency and damping constants were selected in the following manner. The reference natural frequency was set at $f_{ref} = \omega_{ref} / 2\pi = 5$ Hz. The reference viscous damping was selected to cause the exponential envelope of response to decay to 2% of its initial value within 1 sec when no Coulomb damping is present. Thus, the reference viscous damping ratio is found by $\zeta_{ref} = -\ln(0.02)/\omega_{ref} = 3.912/\omega_{ref}$. Evaluating this equation at $\omega_{ref} = 10\pi$ rad/sec gives $\zeta_{ref} = 0.1245$.

Similarly, the reference Coulomb damping was selected to cause the linear decay envelope of response to decay to 2% of its initial value within 1 sec when no viscous damping is present. For $f_{ref} = 5$ Hz, exactly five full cycles are completed within 1 sec. From Eq. (4) with $\zeta = 0$, the peak absolute displacement drops $2x_k$ each half-cycle, so we calculated x_k from $X_0 - 10\times 2x_{k-ref} = 0.02X_0$. This gives the reference Coulomb step displacement $x_{k-ref} = 0.049X_0$.

Numerical simulation was used to address important issues characteristic of experimental measurement. For free vibration of a system, the number of significant samples and the sampling rate are limited by the magnitude of damping and by the data acquisition system. Further, no data acquisition is free of error, due to sources such as digital quantization and electrical noise. Both sampling and experimental error (in the form of simulated noise) were considered in this analysis. Through simulation, the accuracy of the method may be assessed easily because the correct result is known before the method is applied. For a selected set of parameters, the simulated response to initial displacement was calculated from Eqs. (3), (4), and (5). (In the numerical simulations, values X_0=1 and x_ε=0 were fixed, so these quantities were not minimization parameters.) Then LSQCURVEFIT was used with the simulated data to identify parameters ζ, x_k, and ω_n. The differences between the identified parameters and the originally specified "true" values provided an assessment of the accuracy of the method.

The curve-fitting method was tested with viscous damping alone ($x_k = 0$) and with Coulomb damping alone (ζ=0) to investigate the method's effectiveness at decoupling the two forms of damping and to determine the residual error in the excluded damping parameter. For the case of viscous damping alone, the method was tested with true values ω_n=10 π rad/sec and $\zeta = 0.81\ \zeta_{ref} = 0.1$ for noise-free data and for data with 1, 3, and 5% simulated noise. The noise was computed by a random-number generator as a normal distribution of zero mean and unit standard deviation, then multiplied by 1, 3, or 5% of the initial displacement, and it was added to the perfect simulated data to form a typical noisy signal. An example of each level of noise may be seen in Fig. 1.

The data were generated in MATLAB for free vibration resulting from unit initial displacement and zero initial velocity, ($x(0)$=1, $\dot{x}(0)$=0). Simulated data sampled at increments of 0.005 sec over an interval of 1.5 sec were computed to represent a typical measured signal. The least-squares curve-fitting method was applied to one hundred different simulated free-vibration decays, and the results were averaged to remove any biases from "less noisy" or "more noisy" signals due to randomness of the simulated noise. The results for viscous damping alone, as displayed in Table 1, indicate that the method was successful in decoupling the two forms of damping. For noise-free simulated data, Table 1 indicates nearly zero residual Coulomb damping and nearly zero error for the viscous damping ratio. Furthermore, the table indicates that even with the presence of 3% random noise, the estimated viscous damping ratio deviates from the true value by only 1%. The predicted natural frequency is quite good as

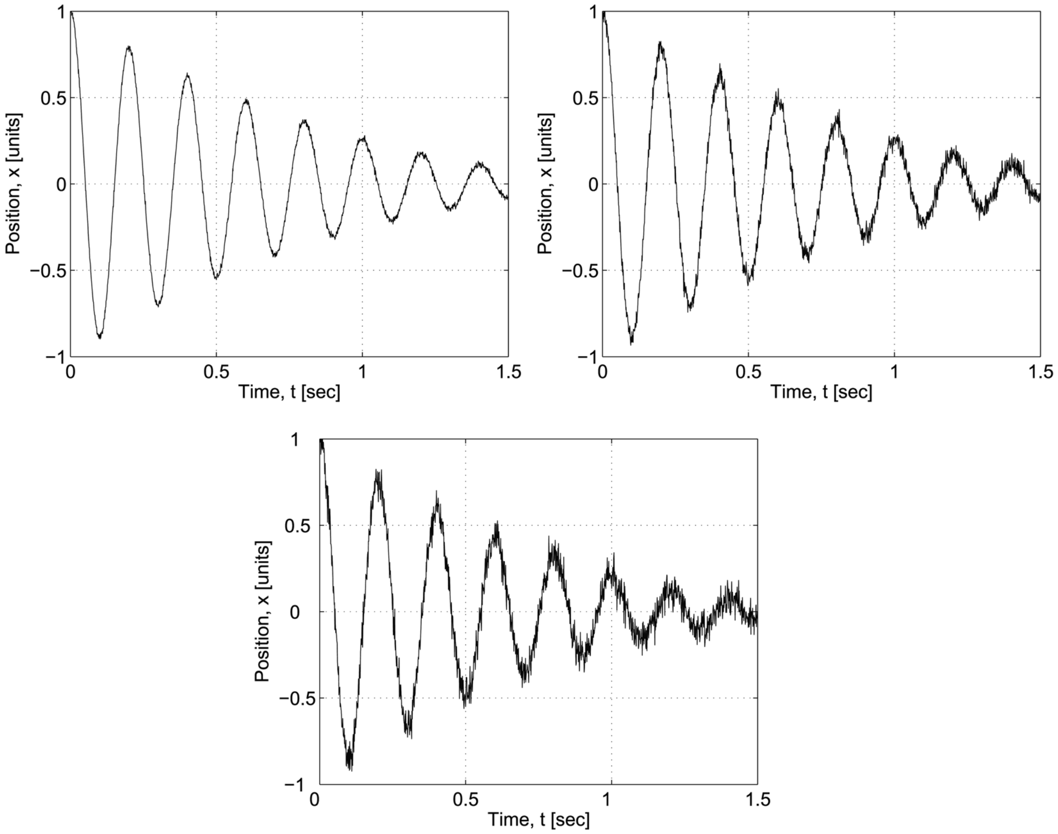

Fig. 1 Examples of response with 1, 3, and 5% random noise included for a system with 5 Hz natural frequency and with viscous damping ratio $\zeta = 0.03$ and Coulomb step displacement $x_k = 0.01$ units

Table 1 Accuracy of least-squares curve-fitting analysis for natural frequency and viscous damping, with no Coulomb damping included in the simulated system, sampled at 200 Sa/sec for 1.5 sec; $\zeta_{ref} = 0.1245$ and $x_{k\text{-}ref} = 0.049$ unit

True value	Average Error or Residual	0% Noise	1% Noise	3% Noise	5% Noise
$f_n = f_{ref} = 5$ Hz	Frequency Error [%],	3.9×10^{-12}	2.7×10^{-2}	8.6×10^{-2}	1.42×10^{-1}
$\zeta = 0.81$ $\zeta_{ref} = 0.1$	Viscous Damping Error [%]	1.9×10^{-8}	3.6×10^{-1}	1.0×10^{0}	1.91×10^{0}
$x_k = 0$	Coulomb Damping Residual $x_k/x_{k\text{-}ref}$	7.8×10^{-9}	2.0×10^{-3}	5.9×10^{-3}	1.1×10^{-2}

well for all levels of damping.

The curve-fitting method was also applied to a simulated system with Coulomb damping alone. Simulated noise was generated by a random-number generator, multiplied by 1, 3, or 5% of the initial condition, and added to the perfect data to produce simulated noisy signals. Data at increments of 0.005 sec over an interval of 1 sec were computed to represent a sampled signal. The method was applied for one hundred signals, and the results were averaged. The results from this process, as displayed in Table 2, indicate very little residual viscous damping. Furthermore, the Coulomb damping value was estimated

Table 2 Accuracy of least-squares curve-fitting analysis for natural frequency and Coulomb damping, with no viscous damping included in the simulated system, sampled at 200 Sa/sec for 1.0 sec; ζ_{ref} = 0.1245 and $x_{k\text{-}ref}$ = 0.049 unit

True value	Average Error or Residual	0% Noise	1% Noise	3% Noise	5% Noise
$f_n = f_{ref}$ = 5Hz	Frequency Error [%]	6.8×10^{-12}	3.3×10^{-3}	7.2×10^{-2}	1.4×10^{-1}
$x_k = 1.02x_{k\text{-}ref}$ = 0.05	Coulomb Damping Error [%]	8.1×10^{-5}	9.7×10^{-1}	2.4×10^{0}	4.9×10^{0}
ζ = 0	Viscous Damping Residual ζ/ζ_{ref}	3.8×10^{-7}	7.1×10^{-4}	1.6×10^{-3}	3.7×10^{-3}

very accurately from noise-free data. For data with 1% simulated noise, the results indicate only a 1% difference between the estimated and true Coulomb damping values. For the 5% simulated noise, the results indicate a nearly 5% error in the Coulomb damping value. Thus despite significant noise, there is relatively little error in the estimated parameters.

Theoretically, only three samples are required for the least-squares curve-fitting method in this simulation study, in which case the minimization equations become a single system with three unknowns, ω_n, ζ, and x_k. However, it is clear that many more samples are required to represent a full vibration-decay record. The effect of sample size was tested by determining the average percent difference in the parameters associated with a given sample length at a sampling rate of 800 Sa/sec. Sample lengths of 154, 311, 462, 619, 772, 927, and 1081 data points were examined, corresponding respectively to 1, 2, 3, 4, 5, 6, and 7 complete cycles of damped vibration. Both numerically perfect simulated data and data with simulated noise of 1% of the initial displacement, as described previously, were considered. The numerically perfect data showed nearly zero differences in the estimated parameters for all sample periods tested. For the case of 1% simulated noise, Fig. 2 shows that error decreases as the sample size increases. Fig. 2 suggests that accurate estimation of the damping constants requires data from as many cycles of vibration decay as possible.

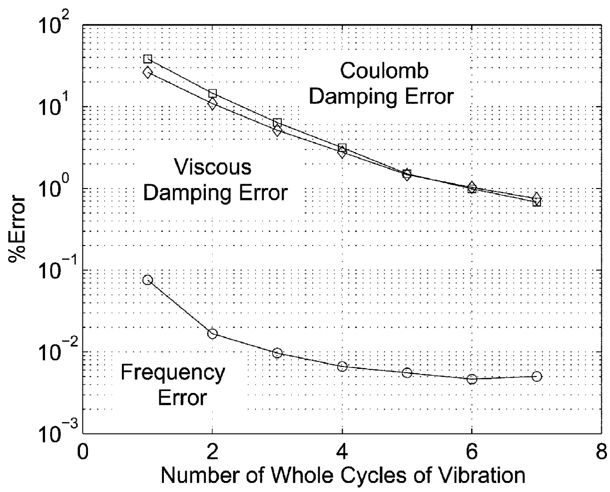

Fig. 2 Effects of sample size on errors in estimated parameters for a simulated system with true values ω_n = 10π rad/sec, ζ = 0.02, and x_k = 0.02 unit, and with 1% simulated noise. Sampling rate = 800 Sa/sec.

3.2. Experiments with a laboratory mass-spring apparatus

The apparatus was a Model 210a Rectilinear Plant purchased from Educational Control Products (ECP) of Bell Canyon, California, USA. Figure 3 is a photograph of the mechanical portion of the ECP 210a used for the present study. The complete ECP 210a can be configured as a 1-, 2-, or 3-DOF mass-spring system. The following description is taken from the user's manual (Parks 1999): "The apparatus ... consists of ... three ... mass carriages interconnected by bi-directional springs. The mass carriage suspension is an anti-friction ball bearing type with approximately ±3 cm of available travel. The linear drive is comprised of a gear rack suspended on an anti-friction carriage and pinion ... coupled to the brushless servo motor shaft."

An optical encoder measures the position of each mass carriage: a pulley is attached to the encoder shaft, and a taut wire attached at the front and back ends of the mass carriage is wound in a loop around the pulley, thus converting translation of the mass carriage into rotation of the encoder shaft. One complete rotation of the shaft produces 16,000 encoder counts, corresponding to mass-carriage translation of 7.06 cm. Hence, the displacement resolution is 4.41×10^{-4} cm/count, an insignificant quantization step relative to the mass-carriage displacements on the order of a centimeter that we initiated. Acquisition and storage of data is managed by a personal computer that runs ECP software and is equipped with an ECP controller circuit board. For the present study, encoder counts were sampled at increments of 0.000884 sec (sampling rate = 1.131 kSa/sec). Sampling times and encoder counts from each data acquisition were stored in a text file, and these data were subsequently transferred into MATLAB for processing.

We configured the mass-spring apparatus as a 1-DOF system by locking down the second and third mass carriages. The linear drive motor is designed to provide excitation and/or control force to the first mass carriage through the link shown on Fig. 3; however, the drive motor was turned off for the free-vibration motion of this study, so the motor-gear-link combination served only to add parasitic inertia and damping to the 1-DOF system. The inherent passive damping of this system was due presumably to several natural causes, including: rolling of the bearing balls and rubbing against races; parasitic drag from the drive motor and the optical encoder; structural damping in the springs; and aerodynamic drag. Additional masses of nominal values 0.25 kg and 0.5 kg can be attached to each carriage of the ECP 210a, and we used this feature to configure five distinct 1-DOF systems, each with a different vibrating mass and possibly different damping magnitudes due to the different weight on the ball bearings.

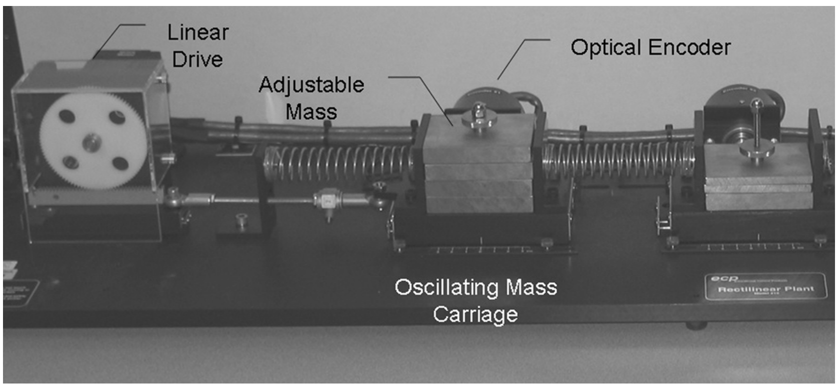

Fig. 3 Photograph of the portion of the ECP 210a mass-spring system used in this study

Our procedure to produce free vibrations by hand was to perturb the first mass carriage into a displacement greater than a centimeter, then to release the mass carriage. In order to eliminate the effects of any inadvertent hand-induced initial velocity, we discarded about the first half-cycle of data. Thus, the data that we analyzed was initialized at the first crest or trough of the vibration decay following the release, at which instant the velocity was closest to zero.

Each free-vibration-decay time series acquired was input to MATLAB's LSQCURVEFIT program along with the M-file algorithm representing the theoretical response of the system, as is described at the end of Section 2. The parameters estimated by the least-squares curve-fitting method are: viscous damping ratio ζ, Coulomb step displacement x_k, natural frequency ω_n, initial displacement X_0, and displacement bias x_ε.

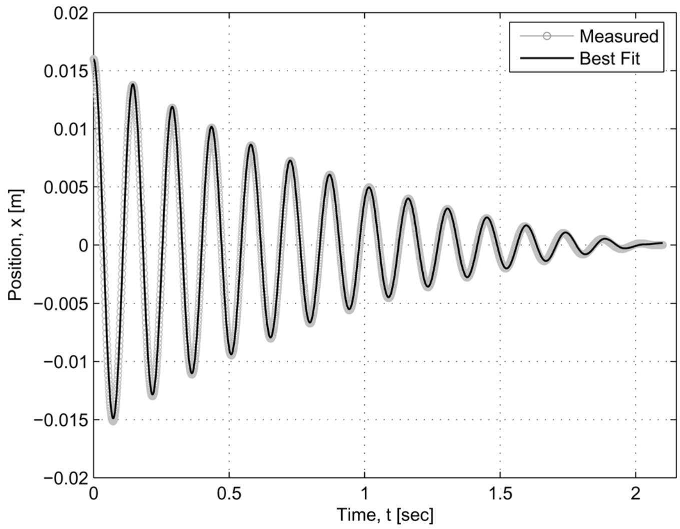

Fig. 4 Measured and best-fit vibration decays of mass carriage with zero added mass

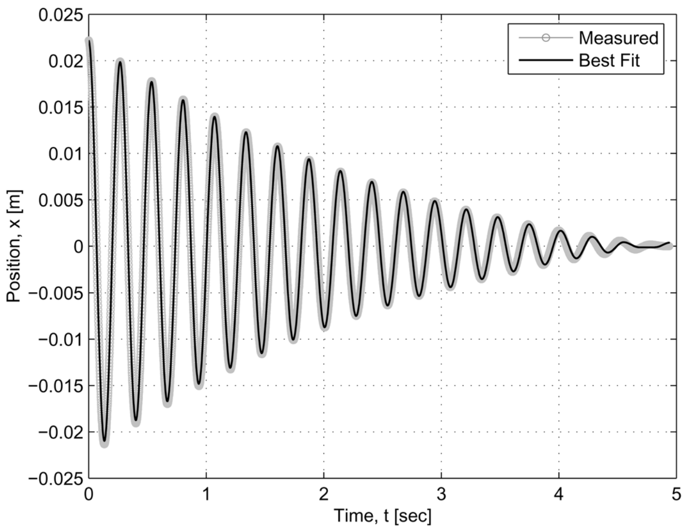

Fig. 5 Measured and best-fit vibration decays of mass carriage with 1.965 kg added mass

Table 3 Resulting parameters for variation in added mass of ECP 210a

Added Mass [kg]	Frequency, ω_n [Hz]	Viscous Damp. ζ	Coulomb Damp. x_k [cm]
0	6.89	0.0184	0.0112
0.2415	6.06	0.0174	0.0112
0.4915	5.45	0.0160	0.0117
0.9835	4.65	0.0144	0.0119
1.4750	4.12	0.0134	0.0121
1.9650	3.74	0.0136	0.0132

The measured and best-fit estimated vibration decays for zero added mass (mass carriage weight only) are shown in Fig. 4, and those for the maximum added mass are shown in Fig. 5. These figures illustrate generally excellent correlation between best-fit response and measured response. We note that the best-fit response deviates from the measured response near the end of the time series at low levels of vibration: the frequency of the measured response increases slightly before motion ceases, behavior that is not modeled by the theory used for curve fitting.

The most significant of the best-fit parameters calculated from free-vibration data for all five values of mass are listed in Table 3. In all cases, the best-fit value for initial displacement X_0 turned out to be almost identical to the initial value of the measured displacement, and the best-fit value for displacement bias x_ε turned out to be extremely small, on the order of 0.007 cm or smaller.

It is relevant to compare the parameter estimations from our curve-fitting method with estimations based upon the same experimental data and calculated from the method of Liang and Feeny (1998) using Eq. (8), as their method is described in Section 2. We analyzed by the Liang-Feeny method our experimental data for the zero-added-mass case, with the following results. The Liang-Feeny average value of ζ over the entire vibration decay is 0.0189 (as compared with our best-fit value of 0.0184), but the local values vary from 0.0106 to 0.0322. The Liang-Feeny average value of x_k over the entire vibration decay is 0.0107 cm (as compared with our best-fit value of 0.0112 cm), but the local values vary from the physically impossible -0.0160 cm to 0.0274 cm. Clearly, our curve-fitting method produces more reliable estimates than the Liang-Feeny method for damping constants over an entire vibration-decay record.

The thoughtful reader might assert that Liang and Feeny's approach of analyzing only data from crests and troughs of a vibration-decay record is preferable to our approach of using all the data, because their method requires much less, and more easily observable experimental data. This would be a reasonable assertion, especially, if the experimental record consisted only of an analog graph as, for examples, from the screen of an analog oscilloscope, or from a figure in a printed report. However, in a situation such as that, fitting of a theoretical model to all the experimental crest and trough displacement values globally would be preferable to the Liang-Feeny approach of calculating local damping values and then averaging these over the entire record. The theoretical model for this global approach consists of Eq. (7), and the equation for crests and troughs, Eq. (4). We tried this global approach using LSQCURVEFIT with only the crest and trough data from the zero-added-mass case, and the resulting best-fit values for ζ, x_k, and X_0 were identical to three significant digits with the corresponding values calculated by considering all the data.

In addition to estimating damping parameters, we applied the best-fit natural-frequency data listed in Table 3 to identify the effective carriage mass $m_{carriage}$ and the stiffness constant k of the 1-DOF ECP 210a system. The natural frequency, ω_n, is defined as ω_n^2 = k/m where $m = m_{carriage} + m_{added}$ is the total

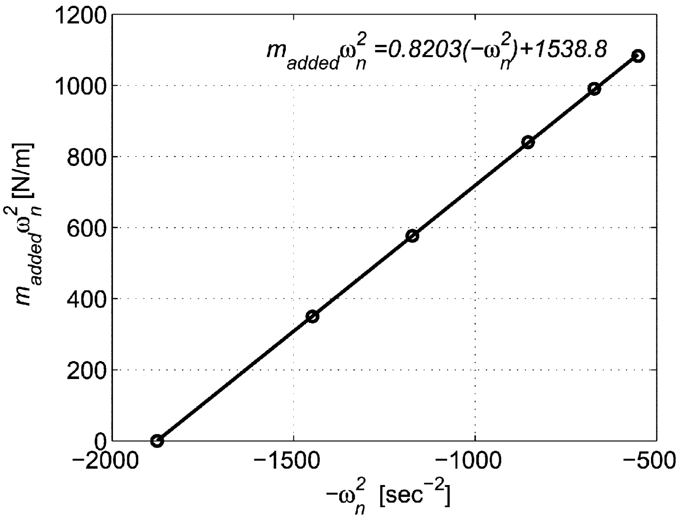

Fig. 6 Determination of carriage mass and spring stiffness from the data in Table 3

vibrating mass. Algebraic manipulation leads to the equation

$$m_{added}\omega_n^2 = m_{carriage}(-\omega_n^2) + k \tag{10}$$

Thus, we can determine the system constants by plotting the five different values of $m_{added}\,\omega_n^2$ versus $-\omega_n^2$, and then fitting a straight line to these data points to calculate best-fit values for slope mcarriage and intercept k, as displayed on Fig. 6. Note that this method is a generalization of the classical added-mass method found in the homework exercises of most textbooks on mechanical vibrations (Meirovitch 2001). The excellent least-squares straight-line fit shown on Fig. 6 gives $m_{carriage} = 0.8203$ kg and $k = 1539$ N/m. To assess the accuracy of these estimated system parameters, we removed the springs from the apparatus shown in Fig. 3, and we measured directly $k = 1546$ N/m. For the ECP 210a apparatus, it is not possible to make an accurate direct measurement of $m_{carriage}$.

4. Conclusions

A method was presented for modeling and identification of a 1-DOF mass-spring system that is damped by a combination of viscous and Coulomb forces. The method uses a least-squares curve-fitting analysis to fit the theoretical model to all of the displacement data measured from a free-vibration decay. The subcritical viscous damping ratio and the kinetic Coulomb frictional force, as well as system natural frequency, are the primary parameters identified from the experimental data.

Numerical simulations demonstrated that the method is successful in decoupling the two forms of damping, leaving nearly zero residual in Coulomb damping when there is only viscous damping in the simulated data, and vice versa. The simulations also indicated that if the data is contaminated by noise, the parameter estimation becomes progressively more accurate as the number of cycles of data retained in the analysis increases.

The method was applied to free-vibration data measured from a laboratory mass-spring apparatus, the mass of which translates on linear bearings that are the primary source of light inherent damping. The quantity of system mass was varied, and free-vibration decays were measured and analyzed for five distinct cases. For two typical cases, the measured and the best-fit-estimated vibration decays were plotted together on the same figure. These figures demonstrate generally excellent agreement of the identified theoretical system with the actual system.

For both the numerical simulations and the experimental study, the damping was light. Thus long samples of multiple cycles were recorded, and the estimated parameters were accurate. Further study is needed to examine the effectiveness of this curve-fitting method when damping is heavier. The method presented here is valid for 1-DOF systems only. The success of this method results from the existence of a closed-form theoretical solution for 1-DOF free-vibration response. Parameter estimation of systems with multiple modes is also a matter of practical importance; however, it is unlikely that there exists a comparable theoretical solution for multiple-degree-of-freedom systems with Coulomb damping. We suggest that a least-squares analysis might still be possible, fitting experimental data to an appropriate numerical solution of the coupled, nonlinear differential equations.

Acknowledgments

We are grateful to: the State Council for Higher Education of Virginia, for financing our purchase of the ECP 210a Rectilinear Plant; Steve Edwards, for providing a great deal of assistance in the laboratory; Scott Bland, for helping with many laboratory tasks, locating key references to previous research, and assisting with the preparation of this paper; Luke Scharf, for recycling and upgrading a personal computer suitable to serve as host for the ECP system.

References

Coleman, T. and Li, Y. (1996), "An interior, trust region approach for nonlinear minimization subject to bounds", *SIAM, J. Optimization*, **6**(2), 418-445.

Den Hartog, J. P. (1931), "Forced vibrations with combined Coulomb and viscous friction", National Applied Mechanics Meeting, June 15-16, *Transactions ASME*, 107-115.

Jacobsen, L. and Ayre, R. (1958), *Engineering Vibrations*, McGraw-Hill, New York, 214-217.

Liang, J.-W. and Feeny, B. (2004), "Identifying Coulomb and viscous friction in forced dual-damped oscillators", *ASME, J. Vib. Acoustics*, **126**(1), 118-125.

Liang, J.-W. and Feeny, B.F. (1998), "Identifying Coulomb and viscous friction from free-vibration decrements", *Nonlinear Dyn.*, **16**(4), 337-347.

Meirovitch, L. (2001), *Fundamentals of Vibrations*, McGraw-Hill, New York, 94-101,103.

Parks, T. (1999), *Manual For Model 210/210a Rectilinear Plant Control System*, Educational Control Products, Bell Canyon, CA. www.ecpsystems.com.

BS